

Analysis of the thermal performance of the novel assembled Chinese solar greenhouse with a modular soil wall in winter of Yinchuan, China

Yanfei Cao^{1,2*}, Hongjun Xu^{1,3}, Miao Shi¹, Xueyan Zhang⁴, Yahong Zhang⁴, Zhirong Zou^{1,2}

(1. College of Horticulture, Northwest A&F University, Yangling 712100, Shaanxi, China;

2. Key Laboratory of Protected Horticulture Engineering in Northwest, Ministry of Agriculture and Rural Affairs, Yangling 712100, Shaanxi, China;

3. College of Horticulture, Xinjiang Agricultural University, Urumqi 830052, China;

4. School of Agriculture, Ningxia University, Yinchuan 750021, China)

Abstract: In order to improve the thermal insulation and storage performance of Chinese solar greenhouses in winter, a novel assembled Chinese solar greenhouse (ACSG) without energy supplement in cold climatic areas was designed to evaluate and compare its thermal performance with that of conventional Chinese solar greenhouse (CSG). The thermal properties of both greenhouses were tested in field on cold winter days in Ningxia, China. The results indicated that the land utilization rate of ACSG was 19.3% higher than that of CSG. On a typical sunny day (the lowest outdoor temperature was -22.0°C) and typical cloudy day (the lowest outdoor temperature was -19.7°C) during the experiment, the minimum indoor temperature of ACSG was respectively 1.7°C and 2.0°C higher than that of CSG. The results for 24 consecutive days (the average outdoor daily minimum air temperature was -19.0°C) showed that the average minimum indoor temperature of ACSG was 1.4°C higher than that of CSG ($p < 0.05$). The modular soil wall attached with colored steel polystyrene boards would be exploited as the north wall of CSG in Yinchuan area.

Keywords: thermal performance, solar greenhouse, north wall, composite wall structure, soil block

DOI: 10.25165/j.ijabe.20221505.6759

Citation: Cao Y F, Xu H J, Shi M, Zhang X Y, Zhang Y H, Zou Z R. Analysis of the thermal performance of the novel assembled Chinese solar greenhouse with a modular soil wall in winter of Yinchuan, China. *Int J Agric & Biol Eng*, 2022; 15(5): 70–77.

1 Introduction

The greenhouse is an agricultural building that can provide appropriate internal micro-climate to grow various crops and plants, shielding them from extreme outdoor weather conditions^[1,2]. Unlike diverse greenhouse types, Chinese solar greenhouse (CSG) holds a cost-effective and energy-saving system. This provides adequate environment to grow warm-season vegetables (e.g., tomatoes, cucumbers, and eggplant) in cold regions of northern China ($32^{\circ}00'\text{N}$ - $43^{\circ}00'\text{N}$) with little or without additional heating, even during the coldest three months of the year with daily average temperature $< -10^{\circ}\text{C}$ ^[3-6]. The total CSG area in China has reached $57.0 \times 10^4 \text{ hm}^2$ in 2019^[7]. CSG has also attracted scientists' interest in other countries attributed to its impressive heat preservation and storage performance^[8-10].

The northern wall plays a great role in load-bearing, heat storage and release, as well as heat preservation and insulation in CSG^[11-13], reducing greenhouse energy consumption by as much as 31.7%^[12]. As materials and thickness of the north wall are

essential factors affecting indoor thermal environment, several researchers have studied numerous wall materials such as soil, clay bricks, gravel, sand, reinforced concrete, phase change materials, and straw^[14-17]. Various studies have demonstrated that the north wall causes heat loss reduction and air environment improvement inside a greenhouse at night^[18,19].

Compared with walls made of other materials, Chinese farmers prefer soil walls due to their good heat preservation and storage performance, straight forward access, and cost-effectiveness. However, soil wall thickness varies considerably. Since the northern wall requires bearing the roof's weight, the cross-sectional shape of soil wall is trapezoidal, whereas the top and bottom widths of the soil wall exceed 2.0 m and 5.0 m, respectively^[20]. The problem with this kind of wall is that it occupies a large area.

In order to realize the light simplification of soil walls, numerous studies have been conducted on CSG in terms of heat storage and release characteristics as well as soil wall thickness^[21-23]. For instance, Huang et al.^[20] divided the soil wall into heat storage and release layer (0.8-1.0 m in thickness), transition layer (2.2-2.6 m thickness), and cold resistant layer (0.4-0.6 m thickness). As a consequence, several research findings demonstrate that the thickness of the effective thermal storage layer is limited to 0.2-0.5 m^[24,25]. Yang et al.^[26] proposed that the optimal thickness of Yangling in Shaanxi, Baiyin in Gansu, Yinchuan in Ningxia, and Tacheng in Xinjiang is 1.0 m, 1.3 m, 1.5 m, and 1.4 m, respectively.

In recent years, various types of active heat storage walls have been investigated in order to simplify the thickness of the wall^[27], such as active-passive phase change wall^[28], active heat storage rear wall^[29], active-passive ventilation wall^[30]. However, with the introduction of active heat storage technology in the wall, the difficulty of wall construction, initial investment, and operation and

Received date: 2021-05-12 **Accepted date:** 2022-01-19

Biographies: Hongjun Xu, PhD, Associate Professor, research interest: facility horticulture engineering, Email: xuhongjun01@163.com; Miao Shi, Master candidate, research interest: facility horticulture engineering, Email: 18846829645@139.com; Xueyan Zhang, PhD, Professor, research interest: facility horticulture, Email: zhangxueyan123@sina.com; Yahong Zhang, PhD, Professor, research interest: facility horticulture, Email: zhyhcau@sina.com; Zhirong Zou, PhD, Professor, research interest: facility horticulture, Email: zouzhirong2005@hotmail.com.

***Corresponding author:** Yanfei Cao, PhD, Associate Professor, research interest: greenhouse structure optimization and thermal environment regulation. College of Horticulture, Northwest A&F University, Yangling 712100, Shaanxi, China. Tel: +86-18821706068, Email: caoyanfei@nwsuaf.edu.cn.

maintenance costs have increased. Another problem is that the load-bearing capacity of the wall has decreased.

Another effective way to reduce soil wall thickness is using insulation material with adequate thickness as wall insulation layer^[31]. Guan et al.^[32] theoretically calculated wall insulation layer thickness for polystyrene plates, leading to optimal insulation thicknesses for CSG north walls in Beijing and Shenyang regions of 6 cm and 7 cm, respectively.

Nevertheless, the soil wall is influenced by its material properties, and its outer surface is easily weathered by wind, sun, rain, and frost heaving, affecting wall structural strength and limiting wall durability^[33]. One of the reasons why soil walls are so thick is to meet the load-bearing requirements. Therefore, another way to simplify the wall thickness is to increase the soil density to improve its bearing capacity. A newly assembled Chinese solar greenhouse (ACSG) using soil block was proposed. It has been confirmed that ACSG has the advantages of low floor space, inexpensive cost, rapid construction, low labor input, straight forward installation, as well as better internal winter thermal environment performance than traditional Chinese solar greenhouse (CSG) as demonstrated in Yangling (34°16'N, 108°06'E), Shaanxi Province^[34,35]. However, works on the applicability of ACSG in cold regions are lacking.

This study was conducted in Yinchuan (38°59'N, 106°33'E), located in the north of Ningxia Hui Autonomous Region of China, indicating temperate continental climate with average low and high temperatures in January of -11.0°C and -1.0°C in 2018, respectively^[36]. The span of traditional solar greenhouse in Yinchuan, Ningxia is usually 7.0-8.0 m^[26,37]. Nevertheless, farmers desire to facilitate indoor mechanized operation, which can be accomplished using higher greenhouse ridge height and larger span.

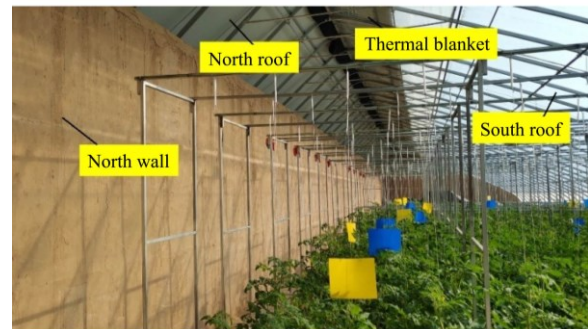
Herein, a new ACSG with a larger space is rationally designed with a wall made up of modular soil blocks and its outside covered with colored steel polystyrene boards. This study aimed to evaluate the thermal performance of the new ACSG compared with that of the local traditional solar greenhouse.

2 Materials and methods

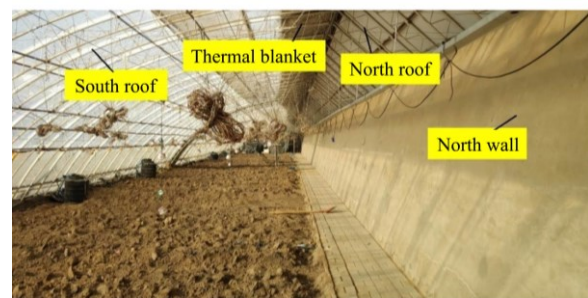
2.1 Experimental greenhouses description

This study is based on two types of solar greenhouses: ACSG with a modular soil wall and local CSG with wall formed through soil accumulation exploited as the control. As presented in Figure 1, solar greenhouses comprise north wall, north roof, south roof, and thermal blanket. The ACSG is 80 m long with east-west orientation, a ridge height of 5.0 m, indoor net span of 10.0 m (outside span of 11.3 m), and a north roof angle of 45° covered with 150 mm thickness colored steel polystyrene board. The effective soil utilization rate is 82.3%. The south roof is covered with 0.10 mm plastic films. The north wall (1.3 m thickness) is a composite wall comprising 1.2 m thick soil blocks and 0.1 m thick colored steel polystyrene boards on the outside. The north wall with 3.7 m height contains three layers of soil blocks with 1.0 m \times 1.2 m \times 1.2 m dimensions. The CSG is 65 m long with east-west orientation, a ridge height of 4.0 m, indoor net span of 7.0 m (an outside span of 10.0 m), and a north roof angle of 45° covered with 150 mm thickness colored steel polystyrene board. The effective soil utilization rate was 63.0%. The south roof is covered with 0.10 mm plastic films. The shape of north wall is physique, with wall upper part 2.4 m wide and the bottom 3.0 m wide. The north wall with 2.5 m height is constructed from soil, and wall inner surface is coated with a cement mortar layer with

10 mm thickness. Both greenhouses' thermal blankets are rolled up to the rooftop during daytime (from 9:00 to 17:30) and spread out (from 17:30 to 9:00 on the next day). The experiment was conducted from December 22, 2018, to March 31, 2019. Tomato was planted in ACSG. Cucumber was grown in CSG, but it was pulled on January 14, 2019.



a. ACSG



b. CSG

Note: ACSG: Assembled Chinese solar greenhouse; CSG: The traditional Chinese solar greenhouse.

Figure 1 Photographs of the experimental greenhouses

2.2 Measurement and data collection system

The measured parameters in greenhouses include indoor and outdoor air temperatures, indoor solar radiation, surface temperature of greenhouse envelopes, soil temperature, and wall temperature. All measurement points inside the greenhouses are presented in Figure 2.

1) Air temperatures of indoor are measured by HOBO UX100-011 recorders (USA, the accuracy of $\pm 0.2^{\circ}\text{C}$, measurement range of -20°C to 70°C). The measurement points are 1.5 m away from the ground inside the greenhouse (points 1, 2). Air temperature outdoor is determined using a HOBO U23-001 recorder (USA, accuracy of $\pm 0.2^{\circ}\text{C}$, measurement range of -40°C to 70°C). The measurement point is 1.5 m away from the ground outdoor.

2) The solar radiation inside greenhouse is measured utilizing a solar radiation sensor (Beijing Huakong Xingye Technology Development Co., Ltd., China, accuracy of $\pm 50 \text{ W/m}^2$, measurement range of 0-1500 W/m^2) connected to a data logger (Juying Electronic, China). The height of measurement point 3 from the ground inside the greenhouse is 1.5 m.

3) The inner surface temperatures of south roof (point 4), insulation blanket (point 5), and north roof (point 6) are measured by means of T-type thermocouples (China, the accuracy of $\pm 0.5^{\circ}\text{C}$, measurement range of -200°C to 260°C).

4) The soil temperatures at depths of 0 mm (point 7), 100 mm (point 8), 200 mm (point 9), 300 mm (point 10), 400 mm (point 11), and 500 mm (point 12) are measured by means of T-type thermocouples.

5) The wall temperatures at depths of 0 mm (point 13), 50 mm (point 14), 100 mm (point 15), 150 mm (point 16), 200 mm (point 17), 250 mm (point 18), 300 mm (point 19), 400 mm (point 20),

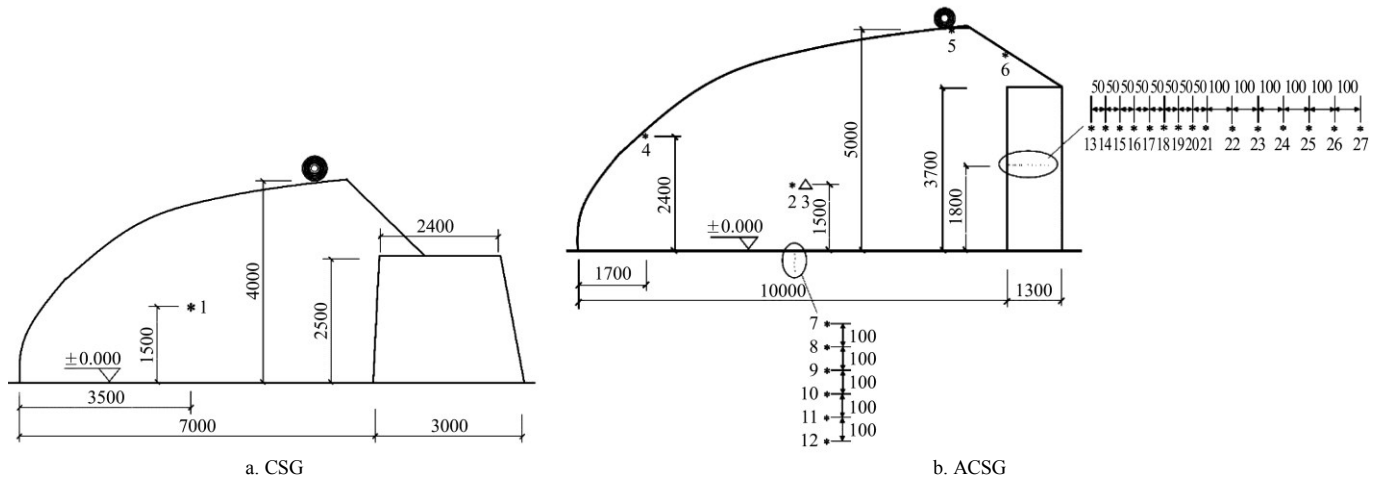
500 mm (point 21), 600 mm (point 22), 700 mm (point 23), 800 mm (point 24), 900 mm (point 25), and 1000 mm (point 26) are determined using T-type thermocouples.

All T-type thermocouples are recorded by means of a data acquisition system (34972A, Keysight Technologies, USA), and obtained data are automatically recorded at 30-min intervals.

2.3 Manufacture of new modular soil blocks

Soil blocks are manufactured from soil (S) and wheat straw

(WS) fiber, with a volume mixing ratio per soil block of S: WS = 1:0.02. The soil block size is 1.0 m (length)×1.2 m (width)×1.2 m (height), as shown in Figure 3a. The manufacturing process is accomplished in 8 min per soil block using a Wall Building Machine (Figure 3b, Shaanxi Yangling Xurong Agricultural Technology Co., Ltd., China). After that, the manufactured soil blocks are transported by forklift trucks for north wall assembly. This method exhibited a rapid construction speed and low labor.



Note: Point 1-2: air temperature recorder; point 3: solar radiation recorder; point 4-27: thermocouple

Figure 2 Distribution of measurement points in all greenhouses



Figure 3 Soil block making and wall assembly process

3 Results and discussion

3.1 Outdoor air temperature

The outside weather data during the test is shown in Figure 4. The outdoor air temperature varies between -24.6°C and 25.0°C during the entire test period. The average outdoor daily maximum air temperature is 9.7°C, the average outdoor daily minimum air

temperature is -13.2°C, and the average outdoor air temperature is -3.5°C. As the date changes from December to the next March, the air temperature gradually increases. The average air temperature in December, the next January, February, and March is -11.8°C, -9.4°C, -3.0°C and 4.6°C, respectively. Therefore, December and the next January are the months that best reflect the performance of solar greenhouse.

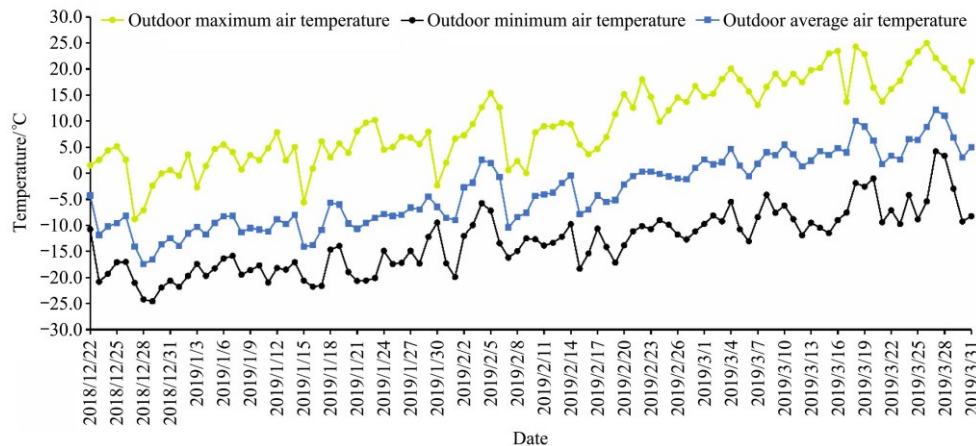


Figure 4 Outdoor meteorological parameters during the test

3.2 Air temperatures inside solar greenhouses

Multiple consecutive days (from December 27, 2018, at 9:00 to January 4, 2019, at 9:00) under cold weather settings were chosen for data analysis, and the hourly air temperatures inside and outside CSG and ACSG and solar radiation inside ACSG are displayed in Figure 5. As presented in Figure 5, air temperatures variation inside ACSG and CSG follow an analogous tendency with outdoor air temperature. In the daytime (9:00-17:00), due to the inconsistency of the ventilation of both solar greenhouses, it is controversial to use the maximum air temperature as an index to evaluate the performance of the solar greenhouse. During the nighttime (17:00-9:00 the next day), the air temperature inside both greenhouses drops slowly due to adding thermal blanket spread on the south roof, augmenting greenhouses insulation. They can best reflect the performance difference between greenhouses. The average air temperatures of ACSG, CSG, and the outside are 10.5°C, 9.6°C, and -13.9°C, respectively. The average air temperature of ACSG was 0.9°C higher than that of CSG. The difference between indoor and outdoor temperatures of ACSG and CSG in the nighttime is 24.2°C and 23.2°C, respectively, which are both higher than 20.8°C in ACSG in Yangling, Shaanxi Province, China^[35]. Both greenhouses meet the requirement of specification evaluation of efficacy for sunlight greenhouse^[38], that is, the required temperature difference between indoor and outdoor at night should be greater than 20°C. Thus, both solar greenhouses

can improve indoor air temperature significantly. Two example days with different weather conditions (sunny or cloudy) were chosen for the data analysis, which are December 29, 2018 (sunny day) and January 3, 2019 (cloudy day). On a typical sunny day (the lowest temperature outside is -22.0°C), the average and lowest air temperatures of ACSG in the nighttime are 6.4°C and 4.7°C, over 0.9°C and 1.7°C higher than those of CSG, respectively. Li et al.^[39] reported that when the outdoor minimum temperature was -18.7°C on a sunny day, the average and lowest air temperatures of CSG in the nighttime in Yinchuan were 6.1°C and 1.1°C, respectively, both of which were lower than those of ACSG. The average and lowest air temperatures of ACSG in the nighttime are 6.0°C and 4.3°C, over 1.2°C and 2.0°C higher than those of CSG, respectively, on a typical cloudy day (the lowest temperature outside is -19.7°C). Li et al.^[39] reported that when the outdoor minimum temperature was -15.8°C on a cloudy day, the average and lowest air temperatures of CSG in the nighttime in Yinchuan were 6.8°C and 2.2, respectively. The average air temperature of CSG is 0.8°C higher than those of ACSG, which may be caused by the fact that the outdoor temperature of ACSG is lower than that of CSG. However, the lowest air temperature of CSG is lower than that of ACSG. Obviously, in the nighttime, the average and lowest air temperatures of ACSG are higher than those of CSG in both kinds of typical weather conditions. This means that the ACSG has a better thermal environment than the CSG.

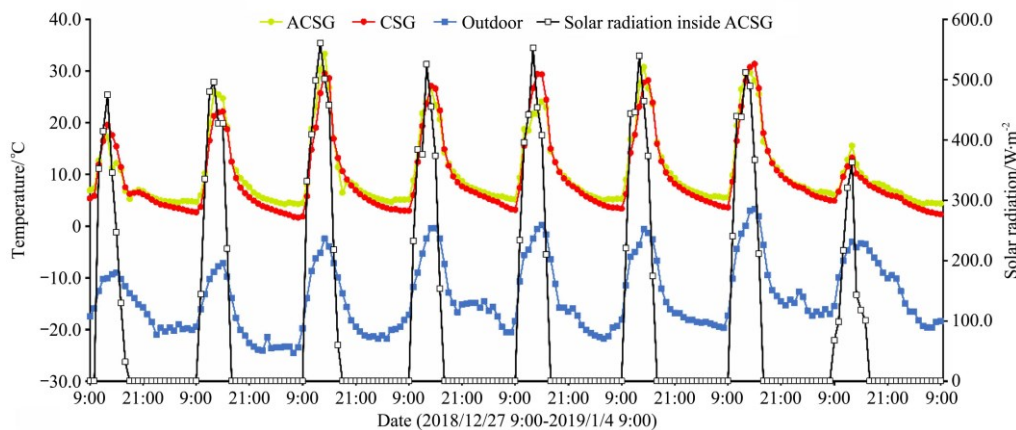


Figure 5 Air temperatures inside and outside two greenhouses (from December 27, 2018, at 9:00 to January 4, 2019, at 9:00)

To compare the long-term thermal performance of two greenhouses, some air temperature parameters are calculated for 24 consecutive days (from December 22, 2018, to January 14, 2019, the average outdoor daily minimum air temperature is -19.0°C), with concluding results as listed in Table 1. The average minimum air temperature inside ACSG is significantly higher than that inside CSG ($p < 0.05$). The average maximum air temperature, average daily air temperature, average daytime air temperature, and average night air temperature inside ACSG are higher than those inside CSG, but the differences are not significant. In addition, since the minimum tolerable air temperature of tomatoes at night is 5°C^[40], the number of days with minimum air temperature $\leq 5^\circ\text{C}$ during the test period in different greenhouses is counted. From Table 1, it can be found that the number of days with minimum air temperature $\leq 5^\circ\text{C}$ inside ACSG is eight days while inside CSG is 17 d. This empowers ACSG to withstand outdoor cold temperatures better than CSG. Hence, the modular soil wall is attached with colored steel polystyrene boards on the outside as the north wall can effectively increase the indoor air temperature at night. However, the suitable temperature range of tomatoes at night is 8°C-13°C, but there are still days when the lowest air

temperature of ACSG is lower than 5°C in winter. The results indicate that there is still insufficient heat in ACSG, and it is necessary to further improve heat storage in order to resist extreme low temperature weather.

Table 1 Indoor air temperatures analysis of two greenhouses (Dec. 22, 2018-Jan. 14, 2019)

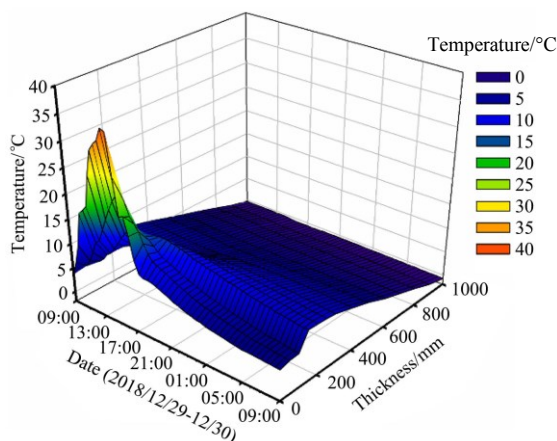
| Parameters | ACSG | CSG |
|--|-----------------------|-----------------------|
| Average minimum air temperature/°C | 5.6±0.2 ^a | 4.2±0.3 ^b |
| Average maximum air temperature/°C | 27.5±0.9 ^a | 26.8±1.2 ^a |
| Average daily air temperature/°C | 11.7±0.3 ^a | 10.9±0.4 ^a |
| Average daytime air temperature (9:00-17:00)/°C | 18.9±0.7 ^a | 18.0±0.9 ^a |
| Average night air temperature (17:00-9:00 next day)/°C | 8.0±0.2 ^a | 7.3±0.3 ^a |
| Number of days with minimum temperature $\leq 5^\circ\text{C}/\text{d}$ | 8 | 17 |
| Number of days with maximum temperature $\geq 25^\circ\text{C}/\text{d}$ | 18 | 15 |

Note: Means with different lowercase letters within a line presented significant differences between the treatments based on Duncan's multiple range test, $p < 0.05$, $n=24$. ACSG: Assembled Chinese solar greenhouse; CSG: The traditional Chinese solar greenhouse.

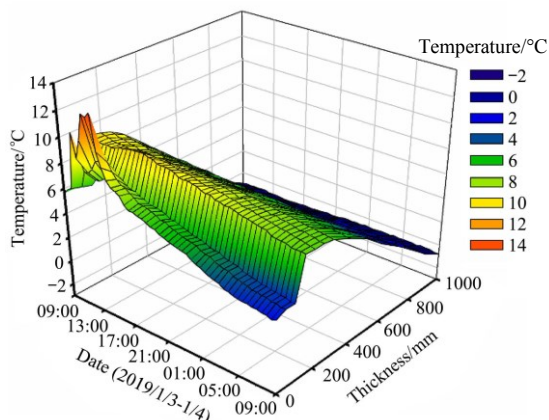
3.3 Temperature distribution of north wall

To evaluate the thermal performance of north wall in ACSG, temperature distribution on sunny and cloudy days is presented in

Figure 6. The results indicate that diurnal variation of north wall surface temperature is similar to indoor and outdoor air temperatures. As demonstrated in Figure 6a, the north wall's inner surface temperature begins to rise after opening thermal blankets at 9:00 on a sunny day, as solar radiation enters the greenhouse and warms the north wall surface. At 14:00, the surface temperature peaks at 35.3°C, higher than other points' temperature inside the wall. The temperature decreases gradually from inner surface to outer surface along with north wall thickness. This implies that the heat gained from north wall's inner surface is transferred to wall interior during daytime. In contrast, during nighttime, the inner surface temperature drops as the heat absorbed by north wall's inner surface during daytime heated the indoor air temperature. Given temperature difference, heat absorbed by the middle layer is conducted to the inner surface of north wall. As a consequence, temperatures of all measuring points inside the north wall start to drop, and that at 200 mm is the maximum among all measuring points. This implies that heat in such an area can be divided into two parts: transferred towards the inner wall surface of greenhouse and the outer wall surface. Based on the results displayed in Figure 6b, analogous conclusions from Figure 6a can be obtained. During a cloudy daytime, the north wall's inner surface temperature peaks at 13:00, with about 12.7°C. Similarly, during cloudy day nighttime, the measuring point with the highest temperature inside the wall is still the measuring point at 200 mm.



a. In the sunny days



b. In the cloudy days

Figure 6 Temperature distribution of modular soil wall inside the ACSG on a typical day during the test

The heat storage capacity of the wall Q_{ws} is defined as,

$$Q_{ws} = \rho_w c (T_{w_17:00} - T_{w_9:00}) \quad (1)$$

where, ρ_w is the density of wall, which is 1940 kg/m³; c is the specific heat capacity of soil, which is 1.84 kJ/(kg·°C); $T_{w_9:00}$, $T_{w_17:00}$ are the average wall temperature at 9:00, 17:00 respectively.

The heat release capacity of the wall Q_{wr} is defined as,

$$Q_{wr} = \rho_w c (T_{w_17:00} - T_{w_9:00 \text{ the next day}}) \quad (2)$$

where, $T_{w_9:00 \text{ the next day}}$ is the average wall temperature at 9:00 the next day.

The average wall temperature T_{w_j} at time j is defined as,

$$T_{w_j} = \frac{\int_0^{y_w} T_{w_y_j} dy}{y_w} \quad (3)$$

where, y_w is the thickness of given wall, which is 1.0 m; $T_{w_y_j}$ is the wall temperature at a specified thickness y at time j .

According to Equations (1)-(3), the heat storage capacity of wall on sunny days (9:00-17:00) and cloudy days (9:00-17:00) are calculated as 5.65 MJ/m³ and -0.44 MJ/m³, respectively. This means that the wall can store 5.65 MJ/m³ of heat during 9:00-17:00 on a sunny day, while the wall needs to release 0.44 MJ/m³ of heat during the same period of cloudy days. The heat release capacity of wall on sunny days (17:00-9:00 the next day) and cloudy days (17:00-9:00 the next day) are calculated as 5.77 MJ/m³ and 3.17 MJ/m³, respectively. The heat storage capacity and heat release capacity of the wall on sunny days are significantly higher than those on cloudy days. Therefore, the wall temperature on sunny days is higher than on cloudy days.

To compare the thermal insulation and heat storage performance of modular soil wall and traditional soil wall, wall temperature data of CSG from literature^[37] and test data of ACSG are selected for comparative analysis, and the results are listed in Table 2.

Table 2 Variations of temperature at different layers of north walls in different greenhouses in January (°C)

| Wall thickness/mm | ACSG | | CSG ^[37] | |
|-------------------|---------------------------------|---------------------------|---------------------------------|---------------------------|
| | Amplitude of temperature change | Average daily temperature | Amplitude of temperature change | Average daily temperature |
| 0 | 17.5 | 11.2 | 10.0 | 12.3 |
| 50 | 10.2 | 10.3 | -- | -- |
| 100 | 5.3 | 8.9 | 5.3 | 11.9 |
| 150 | 2.7 | 11.0 | -- | -- |
| 200 | 1.8 | 10.4 | 2.4 | 12.1 |
| 250 | 1.1 | 9.6 | - | -- |
| 300 | 0.8 | 8.9 | 1.2 | 11.7 |
| 400 | 0.5 | 7.5 | 0.6 | 11.2 |
| 500 | 0.4 | 6.2 | 0.3 | 10.8 |
| 600 | 0.3 | 4.8 | 0.2 | 10.0 |
| 700 | 0.2 | 3.7 | -- | -- |
| 800 | 0.2 | 2.5 | 0.1 | 8.7 |
| 900 | 0.2 | 1.3 | -- | -- |
| 1000 | 0.2 | 0.5 | 0.1 | 7.4 |
| 2300 | -- | -- | 0.1 | -1.1 |
| 2800 | -- | -- | 0.3 | -6.4 |
| 3300 | -- | -- | 5.2 | -11.9 |

The inner surface temperature of north wall changes dramatically. Within a certain wall thickness range, the temperature amplitude decreases gradually with thickness. According to literature^[37], the heat fluctuation layer is proposed to be the area where the amplitude of temperature of indoor side wall in the greenhouse is >0.2°C in a day. The heat fluctuation layer thickness in ACSG wall is 600 mm, which is deeper than

that in CSG wall. After the effective heat storage layer, the average wall temperature decreases continuously with thickness, close to 0°C at a certain thickness (900 mm in ACSG and 2300 mm in CSG). This implies that a composite wall with 300 mm thickness (comprising colored steel polystyrene board with a thickness of 100 mm and modular soil wall with 200 mm thickness) is the same insulation as a traditional soil wall with 1000 mm thickness. Consequently, the modular soil wall pasted with colored steel polystyrene board on the outside exemplifies a potential design improvement for north wall of greenhouse in Ningxia region.

To simplify the analysis, assuming that the wall has a uniform temperature distribution along the length and height, the daily average heat storage capacity of the heat fluctuation layer Q can be estimated by using Equation (4).

$$Q = 24 \sum_{i=0}^d \rho \cdot L \cdot h \cdot w_i \cdot c_p \cdot T_i \quad (4)$$

where, d is the thickness of the heat fluctuation layer, which is 600 mm in ACSG and 500 mm in CSG; ρ is the density of wall, which is 1940 kg/m³ in ACSG and 1710 kg/m³ in CSG; L is the length of the wall, which is 80 m in ACSG and CSG; h is the height of the wall, which is 3.7m in ACSG and 3.3 m in CSG; w_i is

the thickness of the i layer; c_p is specific heat capacity of soil, which is 1.84 kJ/(kg·°C) in ACSG and CSG; T_i is the average temperature of the i layer.

According to Equation (4), the daily average heat storage capacity of the heat fluctuation layer in ACSG is 1.39×10⁶ MJ, while the value in CSG is 1.375×10⁶ MJ. The average heat storage capacity in modular soil wall is a little bigger than that of traditional soil wall. This means that the north wall in ACSG can provide more heat for night air heating than that in CSG.

3.4 Soil temperature

Figure 7 depicts the soil temperatures at different depths on sunny and cloudy days. Both Figures 7a and 7b have implied that soil surface temperature exhibits significant variation over a day. As temperature amplitude decreases with depth, peak temperature appearance also lags with depth. According to Wenbo method^[25], the range of soil temperature change is within 1°C at a depth of 200 mm so that the soil temperature remains fixed, and this depth is considered for the soil effective heat storage layer. This result is smaller than reported^[16], with a 400 mm depth. This is because tomatoes are grown strongly during the experiment, the leaves block most of sunlight, and heat absorbed by soil surface in daytime is relatively small, so the soil depth affected is also quite small.

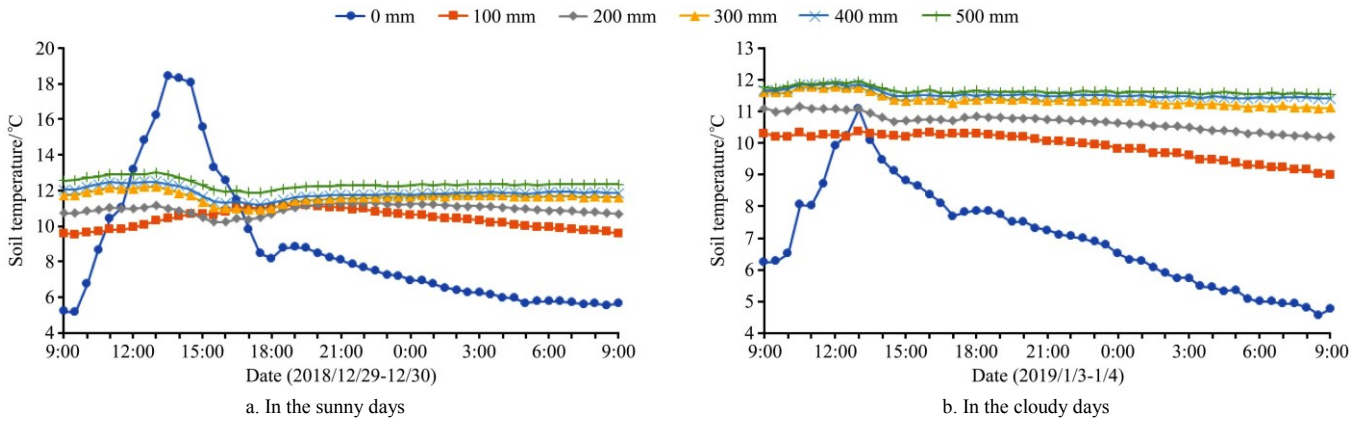


Figure 7 Soil temperatures at different depths inside the ACSG on a typical day during the test

The heat storage capacity of the soil Q_{ss} is defined as,

$$Q_{ss} = \rho_s c (T_{s_17:00} - T_{s_9:00}) \quad (5)$$

where, ρ_s is the density of soil, which is 1710 kg/m³; c is the specific heat capacity of soil, which is 1.84 KJ/(kg·°C); $T_{s_9:00}$, $T_{s_17:00}$ are the average soil temperature at 9:00, 17:00 respectively.

The heat release capacity of the soil Q_{sr} is defined as,

$$Q_{sr} = \rho_s c (T_{s_17:00} - T_{s_9:00 \text{ the next day}}) \quad (6)$$

where, $T_{s_9:00 \text{ the next day}}$ is the average soil temperature at 9:00 the next day.

The average soil temperature T_{s_j} at time j is defined as,

$$T_{s_j} = \frac{\int_0^{y_s} T_{s_y_j} dy}{y_s} \quad (7)$$

where, y_s is the thickness of given soil, which is 0.5 m; $T_{s_y_j}$ is the soil temperature at a specified depth y at time j .

According to Equation (5)-(7), the heat storage capacity of soil on sunny days (9:00-17:00) and cloudy days (9:00-17:00) are calculated as 1.06 MJ/m³ and -0.21 MJ/m³, respectively. This means that the soil can store 1.06 MJ/m³ of heat during 9:00-17:00 on a sunny day, while the soil needs to release 0.21 MJ/m³ of heat during the same period of a cloudy day. The heat release capacity of soil on sunny days (17:00-9:00 the next day) and cloudy day

(17:00-9:00 the next day) are calculated as 1.23 MJ/m³ and 2.50 MJ/m³, respectively. The heat storage capacity of the soil on sunny days is significantly higher than that on cloudy days. However, the heat release capacity of the soil on sunny days is smaller than that on cloudy days. This means that the soil needs to provide more heat for nighttime heating on cloudy days than on sunny days.

3.5 Inner surface temperature of the ACSG

The temperature variation of all surfaces in ACSG on sunny and cloudy days is presented in Figure 8. As shown in Figure 8a, the sunlight enters the greenhouse through plastic film of south roof after opening thermal blanket at 9:00. As the inner surface of wall and soil absorb solar radiation heat, their temperatures gradually augment. Simultaneously, they emit long-wave radiation so that heat is retained in the greenhouse, and temperatures of air and other objects are risen until 13:00-14:00 to reach the maximum. As solar radiation amount is decreased, the temperature is then dropped. After the insulation is covered at night, the heat stored in the wall and ground during the day continue to radiate to the surrounding area until opening the thermal blanket on the next day. Nevertheless, due to weak solar radiation on a cloudy day, the temperature rise is significantly lower than that on a sunny day (Figure 8b).

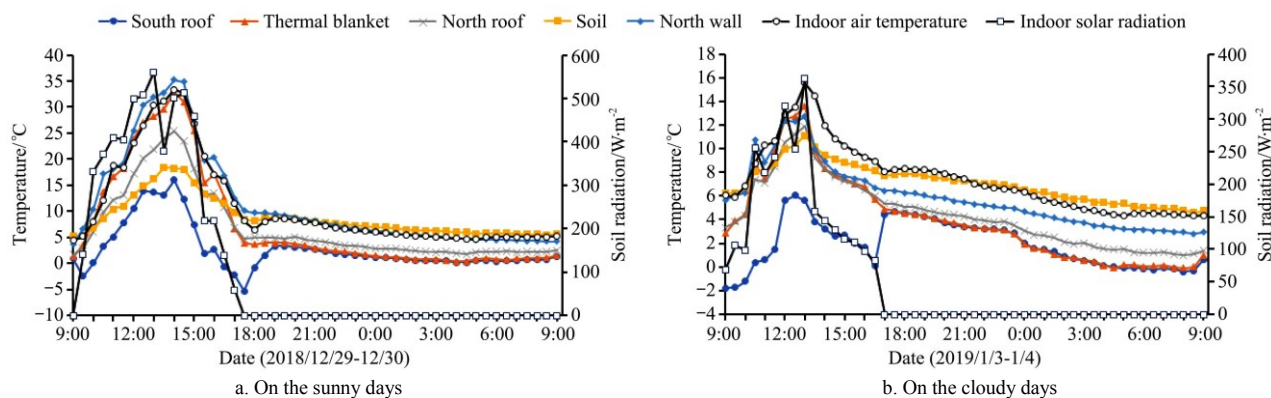


Figure 8 Inner temperatures and solar radiation inside the ACSG on a typical day during the test

4 Conclusions

This study experimentally investigated ACSG with modular soil wall in Ningxia Autonomous Region, China, where the minimum air temperature in winter can reach -20°C or below. ACSG performance was compared with a conventional CSG, and the results indicated that ACSG could replace CSG for winter vegetable production. This study's main findings were: 1) Compared with CSG, ACSG exhibited a higher ridge and a larger planting area, and the land utilization rate of ACSG was increased by 19.3%; 2) On a typical sunny day, the minimum indoor temperature of ACSG was 1.7°C higher than that of CSG. On a typical cloudy day, the minimum indoor temperature of ACSG was 2.0°C higher than that of CSG; 3) The results for 24 consecutive days showed that the average minimum indoor temperature of ACSG was significantly higher than that of CSG ($p < 0.05$). Hence, the ACSG had better thermal capacity than the CSG. The modular soil wall attached with colored steel polystyrene boards on the outside could improve indoor temperature in the nighttime, and could be used to replace the traditional thick soil wall of solar greenhouses in Yinchuan, Ningxia.

Although the current study has some limitations, the results are useful for growers to understand the feasibility of ACSG in cold regions. The present research also shows that wall heat storage and release are essential for creating a favorable environment in solar greenhouse. The next step is to build a simulation model of the greenhouse thermal environment based on crop growth demand, and further discuss the reasonable wall thickness and emergency heating demand of this type of solar greenhouse in different areas.

Acknowledgements

This work was financially supported by the Key R & D Program of Shaanxi Province (Grant No. 2019TSLNY01-03, No. 2021QFY08-02) and the Key R & D Program of Ningxia Autonomous Region (Grant No. 2016BZ0901).

[References]

- Xu J, Li Y, Wang R Z, Liu W, Zhou P. Experimental performance of evaporative cooling pad systems in greenhouses in humid subtropical climates. *Applied Energy*, 2015; 138: 291–301.
- Fernández J A, Orsini F, Baeza E, Oztekin G B, Muñoz P, Contreras J, et al. Current trends in protected cultivation in Mediterranean climates. *European Journal of Horticultural Science*, 2018; 83(5): 294–305.
- Cao Y F, Jing H W, Zhao S M, Zou Z R, Bao E C. Optimization of back roof projection width and northern wall height in Chinese solar greenhouse. *Transactions of the CSAE*, 2017; 33(7): 183–189. (in Chinese)
- Tong G H, Christopher D M, Li T L, Wang T L. Passive solar energy utilization: a review of cross-section building parameter selection for Chinese solar greenhouses. *Renewable and Sustainable Energy Reviews*, 2013; 26: 540–548.
- Wei X M, Zhou C J, Cao N, Sheng B Y, Chen S Y, Lu S W. Evolution of structure and performance of Chinese solar greenhouse. *Jiangsu Journal of Agricultural Sciences*, 2012; 28(4): 855–860. (in Chinese)
- Zhang X H, Chen Q Y, Qu M, Yu F. Heating effects of source heat pump on sunlight greenhouse. *Journal of Shanghai Jiao Tong University (Agricultural Science)*, 2008; 26(5): 436–439. (in Chinese)
- China Association of Agricultural Machinery Manufacturers. *China agricultural machinery industry yearbook 2020*. Beijing: China Machine Press, 2020; 268p. (in Chinese)
- Cao K, Xu H J, Zhang R, Xu D W, Yan L L, Sun Y C, et al. Renewable and sustainable strategies for improving the thermal environment of Chinese solar greenhouses. *Energy & Building*, 2019; 202: 109414. doi: 10.1016/j.enbuild.2019.109414.
- Beshada E, Zhang Q, Boris R. Winter performance of a solar energy greenhouse in southern Manitoba. *Canadian Biosystems Engineering*, 2006; 48: 1–8.
- Ahamed M S, Guo H Q, Tanino K. Development of a thermal model for simulation of supplemental heating requirements in Chinese-style solar greenhouses. *Computers and Electronics in Agriculture*, 2018; 150: 235–244.
- Wang J W, Li S H, Guo S R, Ma C W, Wang J, Jin S. Simulation and optimization of solar greenhouses in Northern Jiangsu Province of China. *Energy & Building*, 2014; 78: 143–152.
- Mobtaker H G, Ajabshirchi Y, Ranjbar S F. Solar energy conservation in greenhouse: Thermal analysis and experimental validation. *Renewable Energy*, 2016; 96: 509–519.
- Sabapathy K A, Gedupudi S. Straw bale based constructions: Measurement of effective thermal transport properties. *Construction and Building Materials*, 2019; 198: 182–194.
- Ma Y H, Li B M, Wang G Q, Liu N, Liu D. Warming and strawberry cultivation effect of building heat storage walls in assembled solar greenhouse. *Transactions of the CSAE*, 2019; 35(15): 175–181. (in Chinese)
- Tong G H, Christopher D M. Temperature variations in energy storage layer in Chinese solar greenhouse walls. *Transactions of the CSAE*, 2019; 35(7): 170–177. (in Chinese)
- Wei B, Guo S R, Wang J, Li J, Wang J W, Zhang J, et al. Thermal performance of single span greenhouses with removable back walls. *Biosystems Engineering*, 2016, 141: 48–57.
- Ling H S, Chen C, Wei S, Guan Y, Ma C W, Xie G Y, et al. Effect of phase change materials on indoor thermal environment under different weather conditions and over a long time. *Applied Energy*, 2015; 140: 329–337.
- Sethi V P, Sharma S K. Survey and evaluation of heating technologies for worldwide agricultural greenhouse applications. *Solar Energy*, 2008; 82(9): 832–859.
- Zhang X, Wang H L, Zou Z R, Wang S J. CFD and weighted entropy based simulation and optimisation of Chinese solar greenhouse temperature distribution. *Biosystems Engineering*, 2016; 142: 12–26.
- Huang X, Wang X F, Wei M, Hou J L, Liu F S, Li Q M, et al. Variation patterns of soil wall temperature and heat flux in sunken solar greenhouse. *Chinese Journal of Applied Ecology*, 2013; 24(6): 1669–1676. (in Chinese)
- Li M, Wei X M, Qi F, Zhou C J. Research progress in wall of solar greenhouses. *Xinjiang Agricultural Sciences*, 2014; 51(6): 1162–1170.

1176. (in Chinese)
- [22] Xu H J, Cao Y F, Li Y R, Alapati, Gao J, Jiang W J, et al. Determination of thickness of thermal storage layer of solar greenhouse wall based on CFD. *Transactions of the CSAE*, 2019; 35(4): 175–184. (in Chinese)
- [23] Shi Y L, Wang X F, Wei M, Li T H, Wang S J. Comparison of Heat Storage and Release Characteristics of Different Thicknesses Soil Wall Solar Greenhouse. *Transactions of the CSAM*, 2017; 48(11): 359–367. (in Chinese)
- [24] Peng D L, Zhang Y, Fang H, Yang Q C, Wei L L. MATLAB simulation of one-dimensional heat transfer and heat flux analysis of north wall in Chinese solar greenhouse. *Journal of China Agricultural University*, 2014; 19(5): 174–179. (in Chinese)
- [25] Li M, Zhou C J, Wei X M. Thickness determination of heat storage layer of wall in solar greenhouse. *Transactions of the CSAE*, 2015; 31(2): 177–183. (in Chinese)
- [26] Yang J J, Zou Z R, Zhang Z, Wang Y B, Zhang Z X, Yan F. Optimization of earth wall thickness and thermal insulation property of solar greenhouse in Northwest China. *Transactions of the CSAE*, 2009; 25(8): 180–185. (in Chinese)
- [27] Luo Q L, Cheng R F, Zhang Y, Fang H, Li D, Zhang J F, et al. Optimization of active heat storage and release system in solar greenhouse. *Transactions of the CSAE*, 2020; 36(17): 234–241. (in Chinese)
- [28] Guan Y, Wang T, Tang R, Hu W L, Guo J X, Yang H J, et al. Numerical study on the heat release capacity of the active-passive phase change wall affected by ventilation velocity. *Renewable Energy*, 2020; 150: 1047–1056.
- [29] Wu Z X, Wang Q, Zhang Y, Zou Z R, Yan L L. Performance test of energy-saving active heat storage rear wall in solar greenhouses in Qinghai. *Chinese Journal of Agrometeorology*, 2020; 41(2): 86–93. (in Chinese)
- [30] Han F T, Chen C, Hu Q L, He Y P, Wei S, Li C Y. Modeling method of an active-passive ventilation wall with latent heat storage for evaluating its thermal properties in the solar greenhouse. *Energy and Building*, 2021; 238: 110840. doi: 10.1016/j.enbuild.2021.110840.
- [31] Li M, Zhou C J, Ding X M, Wei X M, Huang S Y, He Y P. Heat insulation and storage performances of polystyrene-brick composite wall in Chinese solar greenhouse. *Transactions of the CSAE*, 2016; 32(1): 200–205. (in Chinese)
- [32] Guan Y, Chen C, Ma C W, Hu W L, Ling H S, Li D Y. Determination of optimum insulation thickness for solar greenhouse wall. *Xinjiang Agricultural Sciences*, 2015; 52(3): 542–550. (in Chinese)
- [33] Zhou C J. Dr Zhou's investigation titbits (four) protection technologies of solar greenhouse's soil wall. *Agricultural Engineering Technology*, 2011; 6: 32–33. (in Chinese)
- [34] Zou Z R, Bao E C, Shen T T, Chen J. Design and practice of modular assembled solar greenhouse structure. *Agricultural Engineering Technology*, 2017; 37(31): 55–60. (in Chinese)
- [35] Bao E C, Shen T T, Zhang Y, Cao K, Cao Y F, Chen D Y, et al. Thermal performance analysis of assembled active heat storage wall in Chinese solar greenhouse. *Transactions of the CSAE*, 2018; 34(10): 178–186. (in Chinese)
- [36] Historical weather in Yinchuan in January 2018. Available: <https://lishi.tianqi.com/yinchuan/201801.html>. Accessed on [2019-07-15].
- [37] Bai Q, Zhang Y H, Sun L X. Analysis on heat storage layer and thickness of soil wall in solar greenhouse based on theory of temperature-wave transfer. *Transactions of the CSAE*, 2016; 32(22): 207–213. (in Chinese)
- [38] NY/T 1553-2007. Specification evaluation of efficacy for sunlight greenhouse. Agricultural industry standard, Ministry of Agriculture of China, 2007-12-08. (in Chinese)
- [39] Li P, Zhang Y H, Bai Q, Hu W, Jiang L, Zhai X N. Analysis on thermal characteristics of trapezoidal wall based on phase change materials in solar greenhouse. *Chinese Journal of Agrometeorology*, 2019; 40(10): 620–629. (in Chinese)
- [40] Zou Z R, Shao X H. Environmental engineering of facility agriculture. Beijing: China Agriculture Press, 2008; 297p. (in Chinese)